Hindawi

Research Article

Numerical Study to Define Initial Thermal Integration Window for Methane Oxidative Coupling with Dehydroaromatization Reactors

Muhammad Umar Jamil,[1] Maria Haki,[1] Nikolai Nesterenko,[2] Stijn Van Daele,[2] Alessandro Chieregato,[3] and Ma'moun Al-Rawashdeh [1]

[1]*Department of Chemical Engineering, Texas A&M University at Qatar, Doha, Qatar*
[2]*TotalEnergies One Tech Belgium, Parc Industriel de Feluy C, 7181 Seneffe, Belgium*
[3]*TotalEnergies Research Center Qatar, Qatar Science & Technology Park, Al Gharrafa, P.O. Box 9803, Doha, Qatar*

Correspondence should be addressed to Ma'moun Al-Rawashdeh; mamoun.al-rawashdeh@qatar.tamu.edu

Oxidative coupling of methane and methane dehydroaromatization are attractive one-step conversion routes to make valuable platform chemicals more sustainable. Both processes require elevated temperatures above 600°C, good heat management, and the use of heterogeneous catalysts. None of these reactions are yet commercial due to many technical challenges. This work explores the potential of combining these two processes under one umbrella to overcome some of the technical challenges and make these processes more attractive. It focuses on the recuperative autothermal reactor coupling as one of the possible integration options. A tube-in-tube reactor design is proposed in which OCM is in the inner tube and MDA is in the outside. A numerical study is carried out using pseudohomogenous ideal fixed bed reactor models with literature kinetics. A systematic tabulated approach is used to simplify, visualize, and structure the design process and view the design options. Practical constraints such as reactor sizing, pressure drop, reaction performance, and axial temperature profile are investigated. The effect of heat transfer coefficient, diluents, catalyst profiling, and flow direction have been investigated to alter the axial temperature profile, avoid thermal run away, and improve the performance. Multiple thermally coupled OCM-MDA reactor design candidates are identified. This is the first time that the thermal coupling of OCM and MDA has been identified and quantified. These candidates are merely a starting point toward exploring the full coupling opportunities between OCM and MDA toward reaching the ultimate and more attractive option of full mass and heat integration in the same reactor.

1. Introduction

Methane is a major feedstock to produce valuable products such as hydrogen, ammonia, methanol, fuels via Fischer–Tropsch process, and olefins. Today, these processes follow the indirect route in which methane is converted into synthesis gas (CO and H_2), and then is transformed via downstream processing to make the final desired product. Making synthesis gas from methane produces between 9 and 14 kg CO2/kg H2 depending on the source of energy and efficiency of the process. This demonstrates the significant large CO2 footprint that is associated with the indirect route. Direct conversion of methane to valuable products is a promising route that reduces carbon emissions, simplifies the processes, and thus reduces the overall production cost. Some of these highly promising direct methane conversion processes is the oxidative coupling of methane (OCM). Methane reacts with a fractional amount of oxygen at elevated temperatures above 600°C over a heterogeneous catalyst to produce ethane and ethylene as shown in the following equation:

$$2CH_4 + O_2 \longrightarrow C_2H_4 + 2H_2O \left(\Delta H^o = -141 \frac{kJ}{\text{mol of } CH_4} \right).$$

(1)
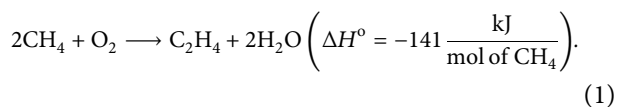
Research on OCM started more than 40 years ago. It has been extensively investigated by academic and industrial groups but has not yet been successfully commercialized. A recent perspective article by Barteau [2] made a complete summary of why is that and suggested research directions toward technology development. The most important challenge to overcome is the strict selectivity versus conversion trade-off associated with this complex reaction scheme caused by the fact that the product (C2+) is more reactive than the feed (CH$_4$). According to multiple studies, the minimum target performance from an industrial perspective is defined when the single pass C2+ yield is larger than 30%. Although thousands of data points from different studies have been populated on the selectivity vs. conversion trade-off, only a few catalysts managed to reach this performance region [3]. According to the analysis by Barteau [2], any efforts directed toward the development of better, i.e., higher yield, OCM catalysts are unlikely to meet with any more success than they have for the past 40 years. A more promising approach for the future is to explore the innovation in the process and reactor design concepts that are economically viable using the existing OCM catalysts. This direction has been explored since the beginning of the OCM development because this reaction is highly exothermic and can form an explosive mixture in the reactor if not properly designed. Multiple reactor designs have been proposed to address this challenge using fluidized-bed, membrane, staged beds with oxygen side feeding, cyclic operation, or feed switching reactors [4]. Another promising direction was to couple the exothermic OCM reaction with an endothermic nonoxidative reaction as a strategy to control the exothermic temperature rise and or boost the yield by further converting the C2+ yield into aromatics or liquid hydrocarbon. Coupling exothermic and endothermic reactions together is a very attractive approach that has been investigated for many other applications [5–8]. This concept is studied the most for methane conversion to synthesis gas and is industrially applied in the case of autothermal reforming [9, 10]. The coupling of exothermic and endothermic reactions can be achieved by (i) direct coupling by carrying out both reactions in the same reactor under adiabatic conditions, (ii) regenerative coupling where the exothermic reaction happened first for a certain amount of time, and then a reverse flow is applied where the endothermic reaction flows for a certain time and this cycle is repeated after that, or (iii) recuperative coupling, which is an indirect coupling where each reaction occurred in a separate channel in countercurrent or cocurrent similar to a heat exchanger reactor. Each of these concepts has its advantages and disadvantages which are nicely summarized in this review work [6].

To better clarify what has been done so far related to the reactor and process integration of OCM with another chemistry, simplified sketches are established in Figure 1(a),

showing all possible integration options at different scales of process, reactor, and catalyst levels. At the process scale as in (i) and (ii), all levels of integration are possible as mass integration, heat integration, or a combination of partial or full integration providing the maximum level of flexibility. At the reactor scale, only two options of integration are possible. Either heat integration as autothermal in (iii) or mass and heat integration as in (iv). At the catalyst scale, only full integration of mass and heat is possible as shown in the two possible options of (v) and (iv).

The first effort to couple the OCM reaction with another chemical reaction started in the 1980s [11, 12]. Since then, a couple of articles are published each year on this topic as shown in Figure 1(b). Reactions that are explored with OCM are shown in Figure 1(b). Apart from the case of Fischer–Tropsch (FT), all reactions coupled with OCM are endothermic reactions operating at a similar temperature as that of OCM and around atmospheric pressure. In this way, the highly exothermic nature of OCM could be controlled by the endothermic reaction. Apart from naphtha, most coupled reactions used methane or ethane as the reactant. Both catalytic and noncatalytic reactions are explored.

Steam methane reforming (SMR) is the most studied coupled reaction. All studies were carried out in different reactor and process concepts such as catalytic membrane, multicatalytic beds, microreactor, and multitubular reactor. Most of the reported work was a modeling study with two experimental validations. One work did a modeling study to couple OCM and SMR at the catalyst scale.

The second most investigated chemical reaction is methane dehydroaromatization (MDA) which is a very attractive direct methane conversion step as the OCM. Methane reacts over a catalyst to produce hydrogen and aromatics, mainly benzene and naphthalene as follows:

$$6CH_4 \longrightarrow C_6H_6 + 9H_2 \left(\Delta H^o = +88.4 \frac{kJ}{\text{mol of } CH_4} \right).$$

(2)
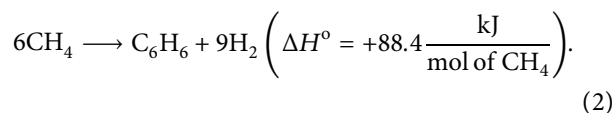
Coupling MDA reaction to OCM was mainly investigated experimentally with combined mass and heat integration in the same reactor with no modeling work till now. The works were mainly driven by the possibility to improve the C2+ yield and improving the MDA catalyst stability as MDA catalyst quickly deactivates and requires continuous regeneration.

The next investigated chemical reactions are related to ethane cracking or ethane dehydrogenation. The most commercially developed OCM technology work by Siluria Technologies (currently Lummus Technology) utilizes ethane and propane cracking as the strategy to maximize the amount of generated C2+ and control the reaction heat [13, 14]. The reported literature work is experimental and involves direct mass and heat integrations in the same reactor. Some effort was carried out to integrate OCM with dry reforming of methane (DRM) via partial mass and heat integration. A nonconventional reactor design was used which used DRM-packed bed membrane reactor integrated into a fluidized bed OCM reactor. The work explored both
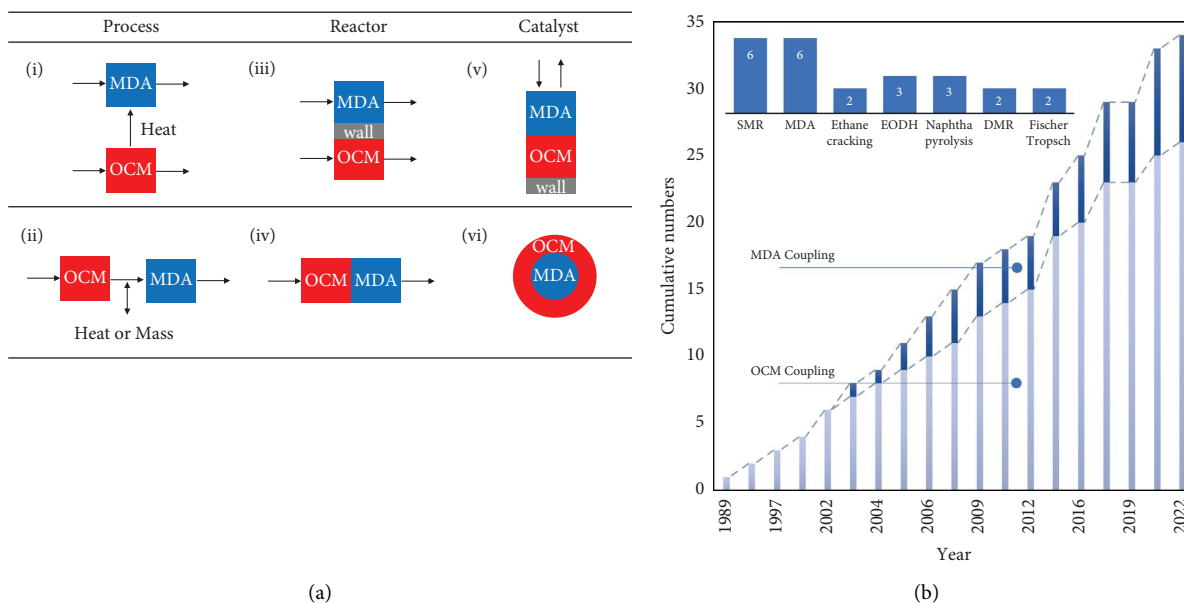
FIGURE 1: (a) Schemes of possible integration options of OCM with NOCM. (i) Heat integration at process scale, (ii) partial mass and heat integration at process scale, (iii) autothermal reactor, (iv) full mass and heat integration at reactor scale, and (v) and (vi) full mass and heat integration at catalyst scale. (b) The historical cumulative number of coupling of OCM with another chemical reaction with emphasis on MDA coupling.

experimental and modeling aspects. The DRM consumed more than 90% of the generated CO_2 in the OCM section and managed to increase the methane conversion of the unreacted methane into valuable synthesis gas products. The work with FT used a membrane in fixed bed and fluidized bed reactors. Here, H_2 and CO passed through the membrane to react with the FT catalyst and form longer-chain hydrocarbons. No experimental work was performed in this work, but was presented as a concept supported by the modeling work.

Of all of the mentioned options, MDA is the most attractive to integrate with OCM. This is because MDA on its own is economically very attractive as it makes high-added value products H_2, naphthalene, and aromatics which is a liquid product that is easy to handle and transport. This is all performed in a single step. Both reactions have similar components and operating conditions which can help to utilize the same infrastructure for either reaction in terms of design, operations, and separations, thereby reducing the overall plant costs. Also, both reactions are direct conversions; therefore, the overall CO_2 emissions per final product could significantly be reduced.

The possibility for thermal and chemical synergies for the coupling of MDA with OCM is promising but it is still in its early stages of development. This limitation originated because the MDA catalyst is not yet compatible with the OCM reaction effluent CO_2, CO, and H_2O. For example, the typical explored Mo-ZSM-5 catalyst is sensitive to the cofeeding amount of these components [15]. That is why earlier experimental work proposed process schemes in which these products could be separated before the effluent is passed to the MDA catalyst [16, 17]. The second challenge is catalyst stability. The MDA catalyst deactivates rapidly in a couple of

hours which requires more frequent regeneration. Achieving this in an integrated OCM-MDA reactor is not straightforward. As well, experimental work carried out on coupling these two chemistries is still at the laboratory scale carried out with excess catalysts. Thus, available knowledge on this integration option so far is still very limited.

This work addresses the reactors integration option via thermal coupling only as a first step toward the full synergy potential of mass and heat integration. In this case, OCM and MDA reactors are coupled thermally and are separated by a dividing wall. The heat requirement of MDA is supplied from the heat released by OCM. Each reaction takes place in a separate reaction channel, which means the reactor effluents do not mix. This significantly simplifies the demand on the catalysts' stabilities and compatibility from each process at this stage. State-of-the-art catalysts can be selected individually for each reactor and replaced as needed. Since both catalysts need to be thermally coupled, the reactor will be operating in nonisothermal mode. Axial and radial temperature profiles will be generated from this integration and it will become particularly critical to how each catalyst will behave. This will define catalyst requirements that can accommodate the temperature variation in a thermally integrated reactor.

This work wants to do a systematic modeling study to better understand the integration space between OCM and MDA in terms of opportunities and limitations. The focus is on thermal integration which serves as the foundation for the more attractive full mass and heat integration in the same reactor. The modeling studies are based on available kinetic models for OCM and MDA that are used to establish separated pseudohomogenous ideal fixed-bed reactor models. Parametric analysis on each reactor will be carried

out to find the required catalysts amounts, operating window, and conditions to thermally couple OCM and MDA in a single autothermal tube-in-tube reactor design. Second, a systematic tabulated approach will be established to define initial reactor design candidates for thermally coupled reactions with acceptable targets. Effects of cocurrent and countercurrent reactor designs, along with catalyst profiling with diluents will be investigated. Diluents are used here as a strategy to control the axial temperature profile and have a bigger operating window away from the thermal runaway. Some sensitivity studies will be carried out to understand critical reactor design parameters, and finally thermally coupled showcases of OCM and MDA will be presented at the end along with recommendations for future work.

2. Mathematical Modeling

The reactor models used in this work were restricted to ideal pseudohomogenous fixed bed reactors. This simplification is acceptable here considering the work objectives are to identify the initial integration operating window and the opportunity to thermally couple OCM and MDA reactions together. First, separated reactor models are established, and then coupled reactors in the form of tube-in-tube arrangement are used as shown in Figure 2. Available kinetic models from the literature are selected for OCM and MDA. The OCM kinetic model from [18] is selected which was developed for 3% Li/MgO catalyst, in the range of 1 atm, 873–1023 K, 1000 cm^3 (STP)/min with the feed compositions of CH_4: 2.5–35% and O_2: 0.12–3.2%. The kinetic model for MDA is taken from [19] which is developed for 6% Mo/HZSM-5 catalyst and was validated for 1 atm, 948–1023 K, 750–3000 ml/g.h with the feed composition of 95% CH_4 balanced with the He as inert. The design equations used in this work are shown in Table 1. Initially, isothermal and isobaric conditions are utilized in the separated reactor study part. Then, nonisothermal and nonisobaric conditions are applied in the coupled tube-in-tube design. No heat and mass transfer limitations were considered and no effect of axial dispersion is considered at this stage. No heat and mass transfer occur with the surroundings.

Based on the reactor model assumptions, the mass, energy, and momentum balance equations were developed as shown in Table 1. The positive and negative signs in the left-hand side of the mass, heat balance, and momentum balance represent the cocurrent and counterflow reactor arrangements, respectively. Q_{ex} is negative for exothermic (OCM) and positive for endothermic (MDA) reactions. The heat transfer coefficients are estimated using different available heat transfer correlations. The pressure drop across the catalyst bed length is estimated using the Ergun equation. While this equation refers specifically to tubular designs, it was used here for the annular geometry, owing to its simplicity. In this work, V_r refers to the total reactor volume occupied by the catalyst volume, V_c, the diluent volume, V_d, and the void space, V_v, and ϵ_c refers to the fraction of the volume occupied by the catalyst particles over the total reactor volume. The set of algebraic and ordinary differential equations is solved using a Python environment (an example of the code used for the coupled reactors model is included in the supplementary
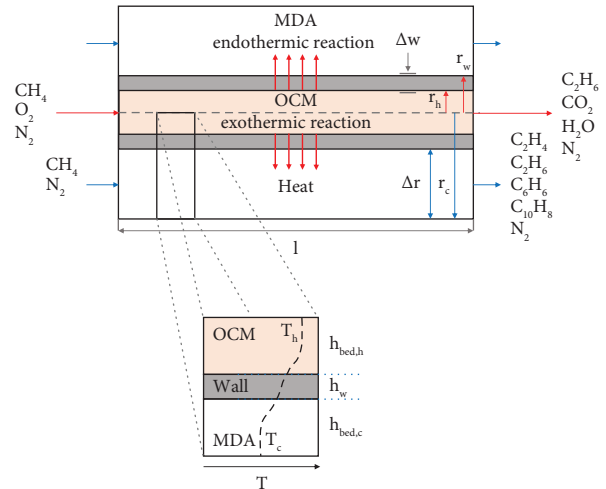

FIGURE 2: Dimensions and schematic of the reactor concept used to develop the mathematical model.

material) by utilizing the required initial and boundary conditions. For all cocurrent simulations, "odeint" command function was used which solves the initial value problem for stiff or nonstiff systems of first order ODEs. For the countercurrent simulations, "solve_bvp" command function was used which solves a first-order system of ODEs subject to two-point boundary conditions. The thermodynamic data are retrieved using Thermochem Package in Python [20].

3. Results and Discussion

3.1. Studies Using Separated Reactor Designs. Parametric studies for OCM and MDA are carried out using their respective fixed-bed reactor models as shown in Table 2. For all the tested conditions with similar inlet flow rates, MDA has lower CH_4 conversion compared to OCM and requires 10 to 30 times more catalyst. Thus, the MDA reactor channel and amount of catalyst are much larger than that of OCM. On the other hand, the amount of heat generated by OCM is much larger than what MDA can consume. To match both reaction heat duties while keeping an acceptable performance, one needs to know what conditions can be adjusted and to what extent. The following guidelines were established based on parametric studies carried out in the conditions listed in Table 2. These guidelines prioritize how the reactor's heat duty is impacted and the reaction performance. Changing the flow rate and amount of catalyst simultaneously adjusts heat duty significantly while keeping the reactor performance fixed. Therefore, this is the ideal first parameter to adjust to match heat duty. The second parameter is the amount of inert used in the feedstock. The amount of inert influences the heat significantly, with a small impact on the reactor performance. The next parameter to adjust is the feed composition. It greatly influences the heat duties but also impacts the reactor performance. The last parameters to adjust are the temperature and pressure as they have a significant impact on performance but a lower impact on the generated heat duty compared to the previous factors.

Table 1: Mass, energy, and momentum balance equations of the reactor model.

Equation type	Equation	Equation number
Mass balance	$(\pm dF_i)/(dz) = \epsilon_c \rho_b A_c r_{i,net}$	(1)
	$r_{i,net} = \sum_j^q r_{j,i}$	(2)
	$\rho_b = m_s/V_r$	(3)
	$m_s = m_c + m_d$	(4)
	$\epsilon_c = V_c/V_r$	(5)
	$V_r = V_v + V_c + V_d$	(6)
Energy balance	$(\pm dT)/(dz) = (Q_g \pm Q_{ex})/(\sum F_i C_{P_i})$	(7)
	$Q_g = \sum \Delta H_{j,i} r_{j,i}$	(8)
	$Q_{ex} = 2\pi r U (T_h - T_c)$	(9)
	$\Delta H_{j,i} = \Delta H_{j,i}^o + \Delta C_{P,j,i}(T - T_R)$	(10)
	$\Delta H_{j,i}^o = \sum H_{f,i}^P - \sum H_{f,i}^R$	(11)
	$\Delta C_{P,j,i} = \sum ((\theta_l/\theta_a) C_{P_l})^P - \sum ((\theta_l/\theta_a) C_{P_l})^R$	(12)
	$U_{overall} = (1/(1/h_h) + (\Delta w A_h/\lambda_w A_m) + (A_h/h_c A_w))$	(13)
Momentum balance	$(\pm dP_n)/(dz) = ((150 \mu/\phi^2 d_p^2)((1-\epsilon_v)^2/\epsilon_v^3)(v/A_{cs}) + (1.75\rho_g/\phi d_p)((1 - \epsilon_v)/\epsilon_v^3)(v^2/A_{cs}^2))(T'T_o)(P_o/P)(F_{To}/F_T)$	(14)

Table 2: Comparison of OCM and MDA parametric studies.

Cases	OCM	MDA
Operating conditions		
Inlet temperature (°C)	700–800	700–800
Inlet pressure (atm)	1–5	1–5
Flowrate (std m³/h)	10,000–20,000	10,000–20,000
Gas hourly space velocity (h⁻¹)	6,900–13,800	831.97–1663.95
Feed composition		
Feed CH_4 mole fraction (%)	45–68.48	50–99
Feed CH_4/O_2 ratio	1.5–5	—
Feed inert mole fraction (%)	10–40	5–50
Reactor performance		
C_2 or C_6 yield (%)	11.4–33.8	0.6–3.0
CH_4 conversion (%)	20.0–46.1	6.4–19.9
O_2 conversion (%)	60.3–99.99	—
C_2 or C_6 selectivity (%)	40.7–73.2	8.6–30.2
Heat and catalyst weight		
Heat requirement (MW)	6.26–13.10	0.72–2.2
Catalyst weight (tons)	0.25–0.5	3.07–6.13

3.2. Systematic Tabulated Approach for Thermally Coupled Reactors. Coupling an exothermic reactor with an endothermic reactor to reach autothermal operation brings much more design complexity than an individual nonisothermal reactor design. Many process parameters are affecting reactor performances. Thus, due to the various factors and possibilities, the identification of an acceptable operating window and proposing optimal reactor design candidates becomes very difficult. A tabulated systematic approach is established here to guide and help navigate between the different design options in a more structured way. A systematic table format is established in three layers, the inputs layer, optimizer layer, and outputs layer, in a table format as shown in Table 3. Here, the optimizer layer is the physical reactor model used to link all the input and output variables together. The inputs layer takes the data from the user and transfers it to the reactor optimizer layer where calculations are performed and correlated, which is then transferred to the outputs layer. The inputs section includes the process operating conditions and design variables. It also includes the constraints for these input variables. Initial values along with the optimization priorities are forwarded to the physical reactor model (the middle section), which is the reactor optimizer. The outputs layer contains all the reactor outlet parameters or the reactor performance parameters such as the conversion, yield, selectivity, and heat duties.

Table 4 shows a step-by-step method on how to fill and operate the reactor coupling approach shown in Table 3. A case study is used to explain that. The targets used in this case study for obtaining the thermal coupling of the reactors as similar heat duty of both reactors ($Q_{MDA} = Q_{OCM}$) are C_2 Yield for OCM ≥30%, O_2 conversion >99%, CH_4 conversion for MDA ≥10%, and similar operating conditions (T, P_{OCM} = T, P_{MDA}). First, the targets, input variables, and constraints are defined based on the user's knowledge learned from the parametric studies and the final targets. A feed flow rate representing a medium-sized plant capacity is used as 10,000 std m³/h for each reactor. The inserts were

kept less than 20% for OCM and 5% for MDA maintained on the lower side for higher productivity. The operating pressure is atmospheric, and the temperature is allowed to be varied between 700 and 800°C which is a common operating window for both the processes. The catalyst amount is an input to the model, but it has no constraint and will be adjusted as needed. The inputs and constraints are added in the input layer as shown in Table 3. After specifying the input parameters and constraints, the desired targets are defined and inserted in the output layer as shown in Table 3. Using the reactor model equations presented in Table 1, the initial output values are calculated and inserted in the output layer. Then, a decision is made upon which reactor will be used as an optimizer. After which, the input variables are ranked as per the optimization priority. The decision of the reactor optimizer and ranking of the variables are based on the guidelines generated from the parametric study. In this study, matching the heat duties is the main objective while maintaining certain constraints. Based on the initial simulated conditions, the generated heat duties for MDA and OCM reactors are 1.15 MW and 9.95 MW, respectively. To match these heat duties, one of the reactor's input conditions needs to be adjusted. Also, a decision needs to be made for either lowering OCM heat duty to that of MDA, making OCM the optimizer and MDA as the target reference, or increased MDA heat duty to that of OCM, making MDA the optimizer and OCM as the target. In this case study, a decision was made to use the MDA reactor as the optimizer while OCM is the reference.

After the reactor optimizer is defined, the ranking of the variables is established. The ranking order is performed to adjust the catalyst weight, feed flow rate, and finally, the inert in the feed based on the learning from the parametric study. The effect of the temperature is investigated first, and then kept fixed as it has a significant influence on the reaction performance. To highlight this priority, the input parameter with the highest optimization priority is placed at the top row as shown in Table 3, whereas the most flexible optimization parameter is placed in the last row of that table.

The next and last step according to Table 4 is to conduct the optimization work. This is started by defining the targets and objective functions, then deciding if single or multiple variables-at-a-time optimization will be utilized. In this work, the optimization was carried out manually as the aim was to understand the coupling space rather than looking for the most optimal solutions. In the future, an optimization algorithm could be used to define the optimal solutions. To do the optimization work, the input parameters were changed as defined by the priority sequence within the given constraints. After adjusting an input, the physical model was used to simulate the new output variable. All the output variables were monitored and compared to the targets and objective function. If at any stage, these targets were reached, the optimization algorithm stops, or else it continues further to the next parameter to be optimized. The proposed approach is structured and helps to visualize what is happening right from the start of setting up the problem towards finally reaching the final optimization results.

TABLE 3: Reactors coupling approach in systematic tabulated format.

Priority	Name	Input layer Units	Initial input	Constraints	Reactor optimizer Optimum values	Name	Units	Output layer Initial output	Optimum output	Targets
OCM					Reference case					
	Inlet temperature	°C	800	800	800	C_2 yield	%	33.8	33.8	>30%
	Inlet pressure	atm	1	1	1	CH_4 conversion	%	46.1	46.1	
	Feed flow rate	Std m^3/h	10,000	10,000	10,000	O_2 conversion	%	99.99	99.99	>99%
	Catalyst weight	tons	0.185	0.185	0.185	Space time	Sec	0.24	0.24	
	Feed methane	%	61.7	61.7	61.7	Heat duty	MW	9.95	9.95	
	Feed ratio	—	3	3	3					
MDA					Optimization case					
1	Inlet temperature	°C	750	T_{OCM}	800	C_6 yield	%	1.1	0.95	
2	Inlet pressure	atm	1	P_{OCM}	1	CH_4 conversion	%	10.3	12.3	>10
3	Feed flow rate	Std m^3/h	10,000	—	72,320	Space time	sec	0.98	0.98	
4	Catalyst weight	tons	3	1–10	10	Heat duty	MW	1.15	9.95	Q_{OCM}
5	Feed inerts	%	5	<20	5	MDA/OCM ratio	—	16.2	54.1	

TABLE 4: A step-by-step chart of how the reactor coupling methodology works with help of Table 3.

(I) Setting up the methodology framework	(II) Define reactor optimizer and variable ranking	(III) Conduct the optimization
(1) Define the input and output parameters of the study	(1) Select which reactor will be used as an optimizer and which reactor as a reference or target	(1) Define the objective function
(2) Select initial conditions and constraints and add them in the input layer	(2) Rank the input variables based on which one to change first	(2) Select single or multivariable-at-a-time optimization
(3) Select targets and add them in the output layer		(3) Carry out the optimization manually or using an automated algorithm
(4) Use the reactor model to calculate initial values for the initial output parameters		

Several results can be generated using the mentioned approach. Some of the achieved results are shown in Figure 3. All of these cases achieved the listed targets for this study. In all of these cases, the following was observed: the required MDA conversion target of 10% was maintained, the coupling temperature was increased, the reactor yields was increased, the required flow rate for MDA was decreased, and the catalyst ratio increased, whereas the heat duties decreased. Each case has a different heat duty, which is an outcome of changing the target temperature. These results are taken as the basis to have a coupled autothermal single reactor design which is a tube-in-tube reactor design with a dividing wall between the OCM and MDA reactor channels.

3.3. Generating Autothermal Coupled Tube-in-Tube Reactor Design Candidates.

In Section 3.2, the metrics from the separated reactors study are compared against each other to match the heat duties. However, these reactors are not yet coupled. Also, the reactor design dimensions and sizing are not yet defined. To develop such a thermally coupled reactor, a tube-in-tube geometry is proposed for this reactor as shown in Figure 2. In such a thermally coupled reactor, the OCM reaction is conducted in one compartment, while the MDA is conducted in a separate compartment. These channels are divided by a wall. The generated OCM heat is transferred to the other compartment to supply the required heat needed by the MDA reaction. For an autothermal operation, no additional heat is supplied or removed from the system. The generated OCM heat should match the heat required by the MDA reaction. In such a coupled reactor design, there is an axial temperature profile that depends on the operating conditions such as flow rates and inlet temperatures and the reactor channel dimensions such as length, diameter, and amount of catalysts. To predict this axial temperature profile and the reactor performance, an energy balance is developed as shown in equation (7) in Table 1. The axial temperature profile (dT/dz) is a function of the heat generated or consumed by the reaction (Q_g); the amount of heat transferred between the channels (Q_{ex}) and the heat capacities (C_P). Equations (10) and (11) show how to calculate Q_g. To calculate the heat exchanged (Q_{ex}), the overall heat transfer coefficient $U_{overall}$ is calculated using equation (13). The local heat transfer coefficient (h_h and h_c) in each channel can be estimated from the existing heat transfer engineering correlations for fixed-bed reactors. Estimating these heat transfer coefficients require prior information about the catalyst particle size, superficial velocity, and channel dimensions (diameter and length). In this work, these parameters are chosen upfront as inputs to the reactor model. Then, the reactor model is used to predict the axial temperature profile and reaction performance for these selected values. These inputs are adjusted until acceptable reactor design targets are achieved. An effort is needed to define an acceptable range for selecting catalyst particle size, superficial velocity, and channel dimensions before proceeding to simulate the coupled reactor.

3.3.1. Selecting Reactors Channels Dimensions, Superficial Velocity, and Catalyst Particle Size.

The equations for pressure drop and the reaction space times are used to define the acceptable ranges for the reaction channels, flow rates, and catalyst particle sizes. Since no mass and heat transfer limitations are considered in this work, no upper bound can be identified for the catalyst particle size. However, the minimum particle size can be directly correlated to the maximum allowed pressure drop. In this work, the pressure drop is estimated using the Ergun equation shown in equation (14) in Table 1. Catalyst particles were assumed to be spherical. To help navigate between the various design options, the Ergun equation is first analyzed as shown in Figure 4(a).

For a given maximum allowed pressure drop (for example, 5% of the inlet pressure), the maximum allowed superficial velocity can be calculated for a given catalyst particle size. For example, if the target pressure drop is set to be lower than 5% of inlet pressure for a catalyst particle of 2 mm, then the maximum allowable superficial velocity in the channel is 1.3 m/s, as shown in Figure 4(a). Exceeding this superficial velocity means the maximum pressure drop limit of 5% will be violated. Therefore, any velocity smaller than this maximum should result in an acceptable pressure drop. For other target catalyst particle sizes and pressure drops, the same approach can be used as shown in Figure 4(a). In this figure, any combination of velocity and catalyst particle sizes below the shown curves is considered an acceptable design.

Using the reaction space-time, a relation can be created between the acceptable superficial velocity and the channel length. This is shown in Figure 5(b) which is carried out for three different space-times. For example, for a given space-time of 0.24 seconds and 0.2–3.5 m/s superficial velocity, the corresponding reactor channel length would be 0.05–0.85 m length.

The next parameters to define are the channel diameter and the number of parallel tubes needed in the reactor to accommodate the total amount of catalyst and the target flow rate. To find these variables, first, the total catalyst volume is calculated from the total catalyst amount and the bulk density. Since the reactor length is already selected, the total reactor diameter can be calculated as shown in Figure 4(c) which is demonstrated for different catalysts amounts, representing different flow capacities. For example, for a flow rate of 10,000 std m³/h, the total OCM catalyst required to reach the target parameters is 185 kgs. For the mentioned 0.05–0.85 m tube lengths, the corresponding total reactor diameters will be 1.2–5 m as shown in Figure 4(c).

The total volume of all the tubes needs to accommodate the total catalyst volume. The total reactor diameter calculated earlier can be split into multiple tubes operated in parallel. In such a case, the reaction channel diameter will decrease and the flow rate per channel will change depending on the total number of tubes selected. Figure 4(d) shows this for different total reactor diameters. For example, if the total number of parallel tubes is 4000, then the tube diameter of each channel will be 2 cm for the case of a 1.2 m
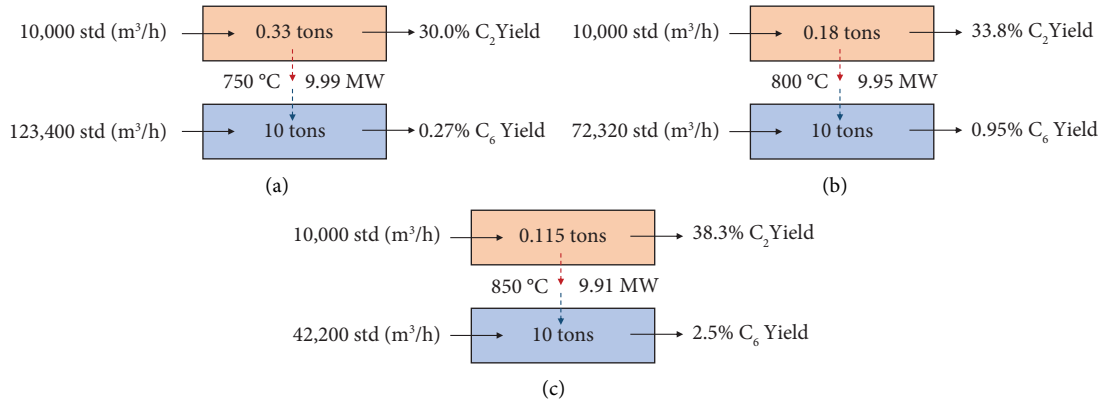
(a)

(b)

(c)

FIGURE 3: Highlights of the final optimization results of the three cases matching the heat duties of both the reactors at three different operating temperatures of 700°C (a), 750°C (b), and 850°C (c). The other targets and constraints are kept the same as in the case presented in Table 3.
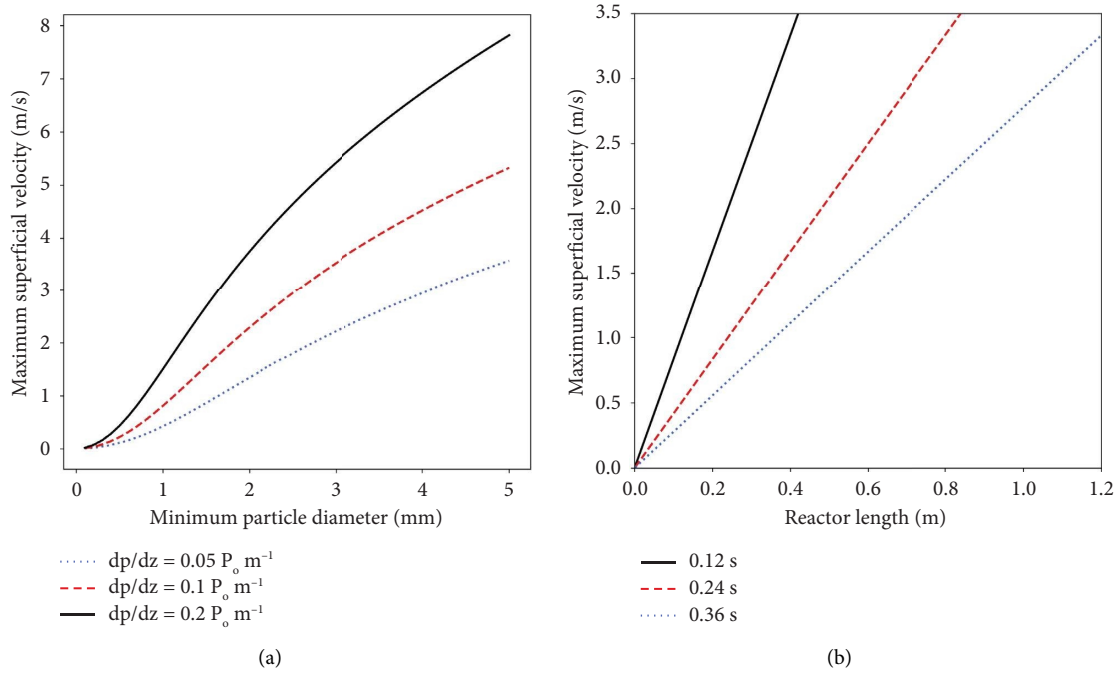

(a)

(b)

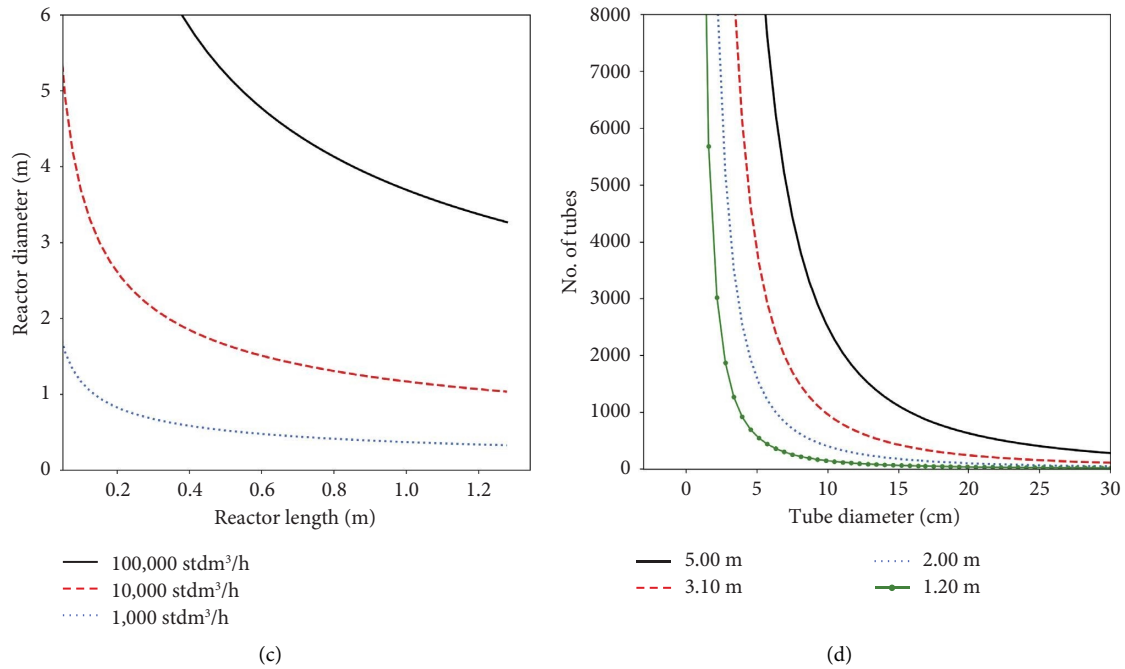FIGURE 4: Continued.

(c)

(d)

FIGURE 4: (a) Maximum superficial velocity for different pressure drop targets, (b) reactor length for multiple space-times shown for $dp/dz = 0.05\ P_{in}$, (c) reactor dimensions for given catalyst weight and 0.24 s space velocity, and (d) number of tubes for multiple total reactor diameters.
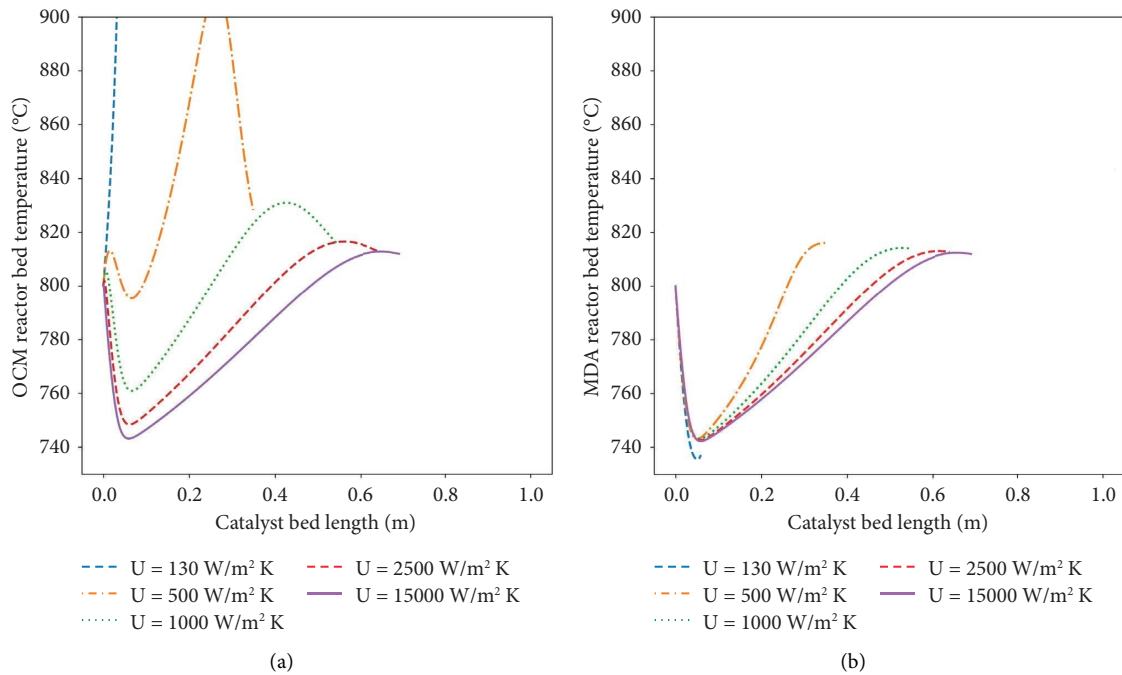

(a)

(b)

FIGURE 5: OCM and MDA temperature profile along the catalyst bed for multiple values of $U_{overall}$ ranging from 50 to 15000 W/m².K.

total reactor diameter. Other combinations can be obtained as needed using the same procedure. It can be noticed that all the abovementioned parameters are highly connected and no single parameter can be adjusted independently. However, we tried to visually represent how to navigate between

all these parameters as shown in Figure 4 to select acceptable ranges for the reactor design and optimization studies.

To proceed further, a reference case is defined which includes the channel dimensions and catalyst particle sizes for OCM and MDA reactor channels as shown in Table 5.

TABLE 5: Base case used for coupled reactor case studies.

	Operating conditions			Feed composition				Reactor design parameters				
	F_{Total}	T_{in}	P_{in}	y_{CH4}	CH_4/O_2	y_{inert}	Space time	L	d_{tube}	Tubes	ε_{gas}	d_p
	Std m³/h	°C	atm	%	—	%	sec	m	cm	—	%	cm
OCM	10,000	800	1	61.7	3	17.8	0.4	1	0.8	20000	50	3
MDA	72,320	800	1	95		5.0	2		6.3		50	3

These data will be used as an initial estimate to design the autothermal coupled OCM-MDA reactor.

3.3.2. Estimating and Defining the Required Overall Heat Transfer Coefficient.

In this section, the U_{overall} is estimated using the operating conditions and reactor channel dimensions presented in Table 5. U_{overall} is calculated using equation 13 shown in Table 1. The heat transfer coefficients for OCM and MDA can be estimated from the heat transfer correlations in the literature for fixed-bed reactors. There are multiple heat transfer models available in the literature for fixed-bed reactors. Some of the common ones are selected and the heat transfer coefficients for OCM and MDA are calculated as shown in Table 6. Conductivity for the catalyst pellet was chosen as 1.2 W/m.K and the feed was taken as pure methane, for simplicity.

Although the same input values are used in all these correlations, there is a significant difference in the estimate of the heat transfer coefficient between these correlations as shown in Table 6. It is not easy to identify which of these correlations provides the best prediction. Computational fluid dynamics and experimentation will be needed to address this question which is outside the scope of this work.

Based on the results shown in Table 6, the heat transfer coefficient for OCM was found to be higher than that of MDA. This is expected as the MDA tube diameter is larger and the velocity is lowered compared to that of OCM. The final U_{overall} for the combined OCM and MDA, in this case, ranged from 4 to 203 W/m².K. Instead of using these predicted U_{overall} values to design the coupled reactor, a decision was made to theoretically vary its value and understand its impact on the reactor design and evaluate when a thermal runaway can occur. In such a way, the minimum acceptable U_{overall} can be identified and also be considered for further studies.

A theoretical analysis was conducted by adjusting the value of U_{overall} between a very low value of 50 and a very high value of 15000 W/m².K. This analysis aims to find out the minimum acceptable heat transfer coefficient which avoids the thermal runaway for the OCM reaction. The exothermic heat that is generated by OCM should be absorbed by the MDA side. If the heat transfer coefficient is not sufficient, the heat generated by the OCM will result in heating the OCM reaction further which will result in thermal runaway. The results of this theoretical analysis are shown in Figure 5. The axial temperature profiles for OCM and MDA are simulated for the mentioned conditions presented in Table 5. For U_{overall} of 500 W/m².K, thermal

runaway is observed with a temperature rise larger than 100°C, whereas for U_{overall} of 1000 W/m².K and above, no thermal runaway is observed and changes in the axial temperature profiles are found to be within an acceptable window. Further increasing U_{overall} beyond 2500 W/m².K does not result in a significant change to the axial temperature profile. Thus, for the current case study dimensions, a target value for the U_{overall} between 1000 and 2500 W/m².K is required to avoid OCM thermal runaway while being within an acceptable design operating window.

For OCM, the maximum predicted value for h_{OCM} is near the targeted values of 1000–2500 W/m².K. While for MDA, the h_{MDA} remains lower than 400 W/m².K which is far below the minimum acceptable range. This means the heat transfer limitation is on the MDA side. The estimated U_{overall} from all the correlations in this study was low. This means the reactor designs with the given dimensions will result in OCM thermal runaway. Thus, the suggested reactor design is not appropriate. To adjust this design, the reactor dimensions and operating conditions have to be adjusted. The first to be adjusted in this design should be the MDA reactor side to increase its heat transfer coefficient. Other strategies to avoid OCM thermal runaway and accept a lower U_{overall} value than 1000–2500 W/m².K are discussed in the following sections.

3.3.3. Using Diluents as a Strategy to Influence the Axial Temperature Profile and Decrease the Minimum Acceptable U_{overall}.

In the previous section, the maximum prediction of U_{overall} using available heat transfer correlation in the literature was 203 W/m².K. This is below the minimum identified U_{overall} of 1000–2500 W/m².K to avoid thermal runaway. Therefore, from a heat transfer perspective, the suggested design parameters in Table 5 are considered unacceptable. There are multiple strategies to avoid thermal runaways. These include proposing alternative reactor design, adjusting reactor channel design, changing operating conditions, side feeding with oxygen, and use of diluent which will be explored further in this work.

The diluent strategy works by mixing the catalyst with diluent material which is an inactive solid particle. Such dilution will minimize the requirement for minimum acceptable U_{overall} to avoid thermal runaway. The downside of using diluents is the reactor volume that increases as the reactor needs to accommodate an additional amount of material. If the diluent is added to both OCM and MDA reactor sides, then the additional required reactor volume can be adjusted by increasing the total number of parallel

TABLE 6: Predicted heat transfer coefficients using multiple correlations from the literature.

Heat transfer models	$h_{h=OCM}$ (W/m^2.K)	$h_{c=MDA}$ (W/m^2.K)	$U_{overall}$ (W/m^2.K)
Leva [21]	44	3	4
De wasch and Froment [22]	160	123	88
Dixon and Cresswell [23]	263	382	182
Tsotsas and Schlünder [24]	945	163	203

tubes in the multitubular reactor. If the diluent is added to either one of the reactor sides, OCM or MDA, some adjustments to the reactor channel diameters are needed besides increasing the total number of tubes in the multitubular reactor; this affects the heat transfer coefficient to some extent.

Figure 6 shows the axial temperature profile for OCM for different cases representing different diluent amounts. In all these simulations, the physical properties of the diluent were assumed similar to the catalyst particles except that the diluent is catalytically inactive. As the diluent amount increases, thermal runaway is avoided using a lower $U_{overall}$ value. When 80% of diluent is used, $U_{overall}$ of 200 W/m^2.K was sufficient to avoid OCM thermal runaway. The temperature profile was similar to the higher heat transfer coefficient, $U_{overall} = 1000$ W/m^2.K with zero diluent. However, the reactor volume increased by 5 times as the total number of parallel tubes increased from 20,000 to 100,000. In all these simulations, the channel diameter and length were fixed and the flow rate per channel was adjusted due to the change in the total number of parallel channels. Thus, the superficial velocity of the OCM reactor was reduced from 2.6 m/s to 0.5 m/s.

If a diluent material is used which has a higher thermal heat transfer coefficient than the catalyst particle, it will help to improve the rate of heat transfer in that channel, thus maximizing the rate of heat transfer. This idea is demonstrated in several studies which show improvement in the rate of heat transfer when using metallic supports due to the improved heat transfer properties [25].

Using diluents enables the possibility to have catalyst profiling in the reactor channel. This influences the axial temperature profile and avoids thermal runaway. Catalyst profiling reduces the amount of the catalyst available in a given reactor volume. This reduces the rate of reaction and the amount of heat generated along the axial dimension. A comparison is made in Figure 7 which shows a homogeneously packed catalyst with 50% diluent versus two catalyst profiling cases. The first is a catalyst profiling from 100% at the reactor channel entrance to 0% near to reaction channel outlet and the opposite case of 0% catalyst at the reactor channel entrance to 100% at the reaction channel outlet. Linear profiling rate is used in both cases. Profiling is carried out separately, first with OCM, and then repeated for MDA. A constant $U_{overall}$ of 700 W/m^2.K was used in all the simulations to allow a fair comparison.

For the OCM case of 0 to 100% profiling, the OCM reaction rate was lowered near the reaction channel entrance, which means less heat was released to the MDA reaction channel side. The temperature profiles for both OCM and MDA were lowered than for the homogenous

case. Only near the reactor exit, the OCM temperature exceeded that of the homogenous case as it has more catalysts. Although different temperature profiles are obtained, similar CH$_4$ conversion is reached for OCM, while the MDA conversion is lowered by 1%. However, the OCM yield shoots up near the reactor exit and the MDA yield shows a slight decrease.

For the other OCM case of 100% to 0% profiling, the OCM reaction rate increases near the reaction channel entrance. As such, the amount of heat that is released to the MDA side increases. The temperature profiles of both OCM and MDA increase in comparison to the case of homogenous mixing. The temperature remains higher for OCM till the exit of the reactor channel then it starts to reduce. This is because the amount of OCM catalyst reduces at that location. This option increases the CH$_4$ conversion of OCM by more than 10% and MDA by 3% in comparison to the homogenous diluent mixing case. The impact is better observed in terms of the yield, where the OCM yield is 28% at the reactor entrance and decreases at the end of the reactor by 24%; however, it remains higher than the yield obtained by the homogenous case, i.e., 15%. And, MDA yield also shows an increase of 0.5%.

A comparison of both catalyst profiling cases of MDA shows a similar trend to that of OCM profiling. When using 100% to 0% MDA profiling, the OCM temperature first drops and then shows a shallow rise. The case was similar to the 50% homogenous case, whereas when the MDA catalyst is decreased along the bed (using 0% to 100% MDA profiling), the OCM and MDA conversion and yields are the best obtained except for the case of 0% to 100% OCM profiling. Although the best OCM and MDA conversions and yields are for 0% to 100% OCM profiling, the 0% to 100% MDA profiling is considered the best scenario from a safety consideration as it has the lowest temperature variation in the axial direction.

In this section, three ideas have been presented to influence axial temperature profile and thermal runaway. The first is the addition of diluents that minimizes the amount of heat generated at a given location in the reactor. This minimizes the need for a very high value of $U_{overall}$ and prevents OCM thermal runaway. Second, using diluents with better thermal conductivity increases the heat transfer coefficient in that reaction channel making the reactor design safer for thermal runaways. Third, catalyst profiling can minimize the variations along with the axial temperature profile and increase the reactor performance such as conversion and yield. Adding diluent in the reaction channels volume allows for generating other design possibilities to control the temperature profile, avoid thermal runaway, and possibly improve the reactor performance. The drawback is that the reactor volume increases.
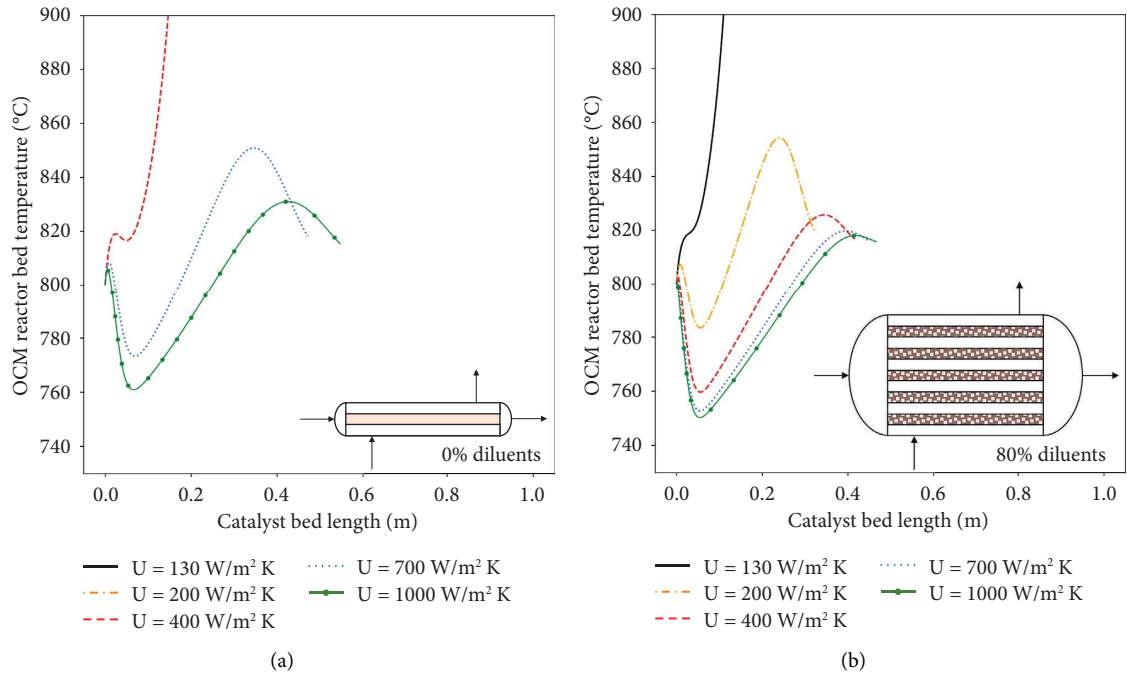
(a)

(b)

FIGURE 6: Effect of adding diluents on the temperature profiles of an OCM-MDA reactor with 0% diluents with $U_{overall} = 400$ and $1000 \, W/m^2.K$ (a) and 80% diluents with $U_{overall} = 130$, 400, and $1000 \, W/m^2.K$ (b).

(a)

(b)

FIGURE 7: Continued.

(c)

(d)

(e)

(f)
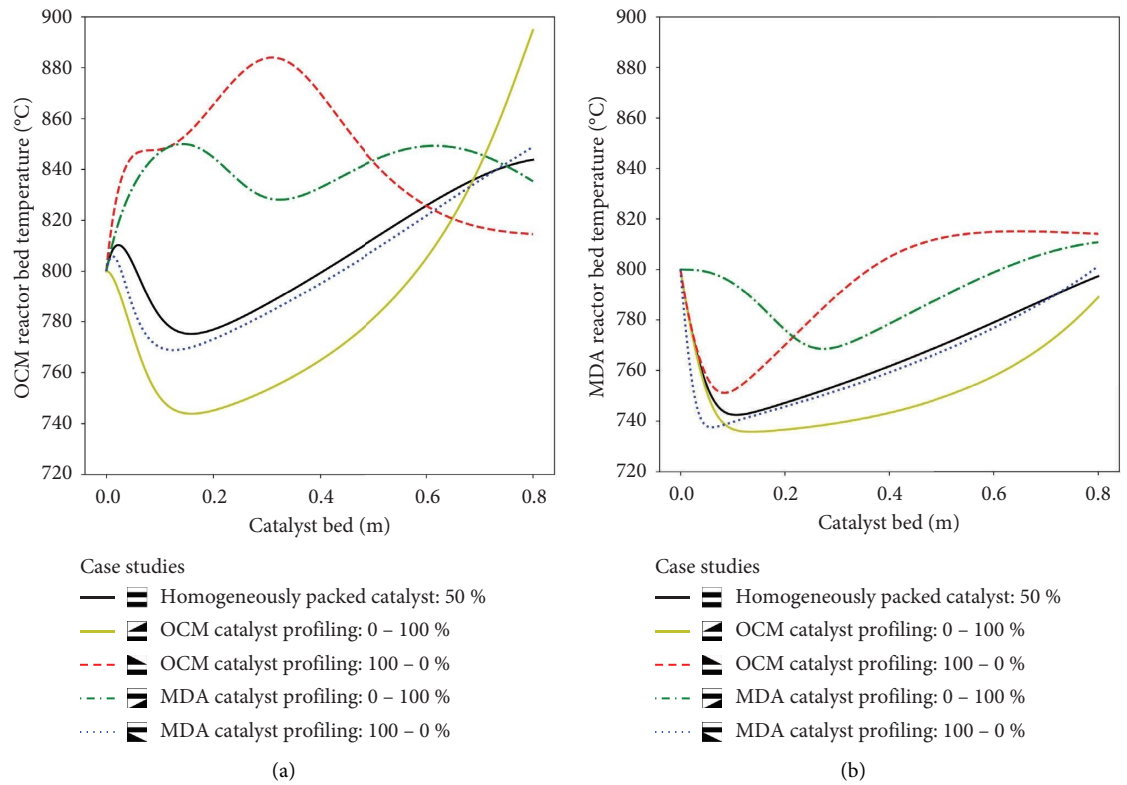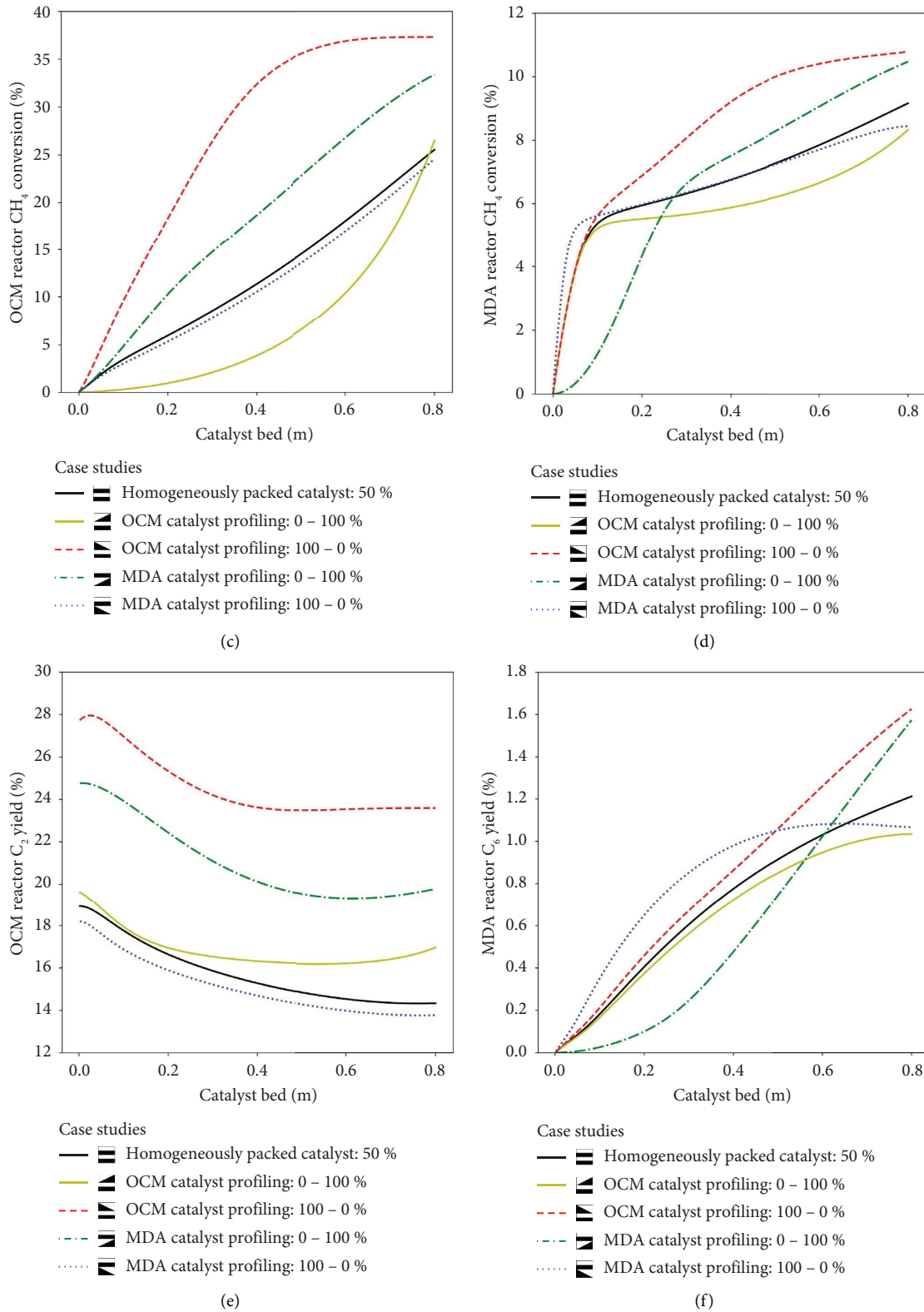
FIGURE 7: OCM and MDA catalyst profiling reactor temperature and performance profiles $U_{\text{overall}} = 700 \, \text{W/m}^2.\text{K}$.

3.3.4. Cocurrent vs Countercurrent Reactor Operation. Operating the reactor as cocurrent or countercurrent influences the axial temperature profile for OCM and MDA as

shown in Figure 8. The conditions shown in Table 5 were utilized in this study except the U_{overall} was purposely chosen as 800 W/m^2.K to better clarify the effect of the coversus

countercurrent operation. For the countercurrent case, there is a steady rise in OCM and MDA temperature profiles with a maximum temperature peak for OCM, whereas when the cocurrent operation is used, the variation in the OCM axial temperature profile is less and with a different temperature profile. The impact on the methane conversion is more than 10% higher for OCM and approximately 2% for MDA for the countercurrent case. A similar increase is observed in the case of yield, 7% for OCM while for MDA a slight increase is observed. According to this study, the cocurrent operation is the optimum option to select, as it helps avoid the possibility of OCM thermal runaway and minimizes the axial temperature variations.

3.4. Autothermal Coupled OCM-MDA Tube-in-Tube Reactor Design Candidates. Based on the conducted studies of diluents, catalyst profiling, and flow direction, findings are identified on how to minimize the axial temperature variations and avoid OCM thermal runaway. First, controlling the overall heat transfer coefficient is a critical design parameter to avoid OCM thermal runaway and approach a sensible reactor design. Adding diluent is a good strategy to lower the demand for heat transfer coefficient, but it increases the reactor volume. Profiling the catalyst by using a diluent is a good method to optimize the axial temperature profile and maximize performance. Using a diluent with higher thermal conductivity increases the heat transfer coefficient which provides better temperature control and minimizes the chances of thermal runways. Optimization is needed to define the optimal catalyst profiling. In the case of MDA and OCM, catalyst profiling on the MDA side from 0% to 100% and cocurrent operation gave the best performance results within an acceptable temperature profile.

Potential candidates for autothermal coupled reactor designs are proposed in Tables 7 and 8 based on the generated learnings. First, some given targets were assumed starting with a high (unrealistic at industrial scale) value of $U_{overall}$ 1200 W/m^2.K. This was selected as a way to initiate the solution search for some design candidates with more realistic $U_{overall}$ values. The maximum pressure drop is less than 20% of the inlet pressure. The maximum variation along with the axial temperature profile (T_{peak}-T_{in}) or (T_{in}-T_{lower}) is lower than 100°C. OCM C2+ yield is at least 30%. MDA CH4 conversion is at least 10%. These targets and constraints are inserted in Table 7 according to the proposed systematic tabulated approach. The initial inlet conditions are filled in the input layer using the same values used in Table 5. The targets are added to the output layer. The constraints are defined based on the learning and studies that were carried out earlier. The first initial reactor outputs were calculated and shown in the output layer. The results are compared to the target and a single variable-at-a-time optimization is performed to adjust the simulation until sensible reactor designs are obtained. Achieving a global optimal reactor design would require implementing an optimization algorithm to map out the entire design space.

Table 8 shows the design outcome for case 1 with a high value for $U_{overall}$. All targets have been met in this case which was used to make more realistic designs with $U_{overall}$ values in the range of 250 and 200 W/m^2.K. Case 2 is the first of these cases. A diluent is added to the OCM catalyst tube as one approach to reduce the minimum required $U_{overall}$ as shown in Figure 6. In this case, the OCM catalyst is diluted by an inert material to have at the end a diluent volume fraction of 48.3% in the OCM reaction channel. As a result, the OCM tube diameter increased from 3.0 cm to 18.4 cm. All other dimensions were kept fixed. All design targets were met using this value of $U_{overall}$.

The reactor design outcome for case 2 will be explained in detail to serve as a basis for all other designs and clarify what are the research gaps that need to be addressed in the future. In this design, the inner tube has the OCM catalyst, while the outer tube has the MDA catalyst in a tube-in-tube reactor design arrangement shown in Figure 2. The OCM inner tube diameter is 18.4 cm while the MDA tube diameter is 25.9 cm. The tubes' lengths are 100 cm. The reaction space-time for OCM is 9.5 seconds while for MDA it is 1.3 seconds. The reached methane conversions are 51.8% and 11.0% for OCM and MDA, respectively. Oxygen is completely consumed. The C2+ yield for OCM is 40.1% while for C6 in MDA, it is 2.0%. The inlet conditions are 800°C and atmospheric pressure for both reactors. If 3000 parallel tube-in-tube units are used, the methane flow capacity that can be processed is 10,000 m^3.N/h and 72,320 m^3.N/h for OCM and MDA, respectively. With these capacities, heat duty that is exchanged between the OCM and MDA reactors is in the range of 9 to 10 MW as shown in the parametric study in Figure 2. This flow capacity requires 123 kg and 6667 kg of OCM and MDA catalysts, respectively. The amount of inert diluent to be added is 3325 kg. The large difference in catalyst amounts demonstrates the large difference in the productivity of these two reactions. The temperature variations in the axial directions (T_{peak}-T_{in}) or (T_{in}-T_{lower})) are around 71 and 60°C for OCM and MDA, respectively, which is considered acceptable according to the set criteria. If both MDA and OCM catalyst particles were spherical and had a catalyst particle diameter of 3 mm, the resulting pressure drop will be less than 1% of the inlet pressure for OCM and MDA, respectively (see Figure 9).

Design cases 3 to 6 are all performed with $U_{overall}$ of 250 W/m^2.K as in case 2, but the channel length, diameters, and number of tubes have been changed while using the same amount of catalyst materials and total flow rates. Case 3 has a shorter tube length of 50 cm and 2000 tubes. Case 4 has a longer tube length and a smaller number of parallel tubes of 500. Case 5 has the shortest channel length of 25 cm, but 10000 parallel tubes. Case 6 has a long channel tube of 200 cm and 2000 tube diameters. In all these design cases, the same performance as case 2 has been achieved. Thus, all designs can be considered acceptable design candidates. Another way to view this result is that the reactor model used in this work is unable to discriminate between these
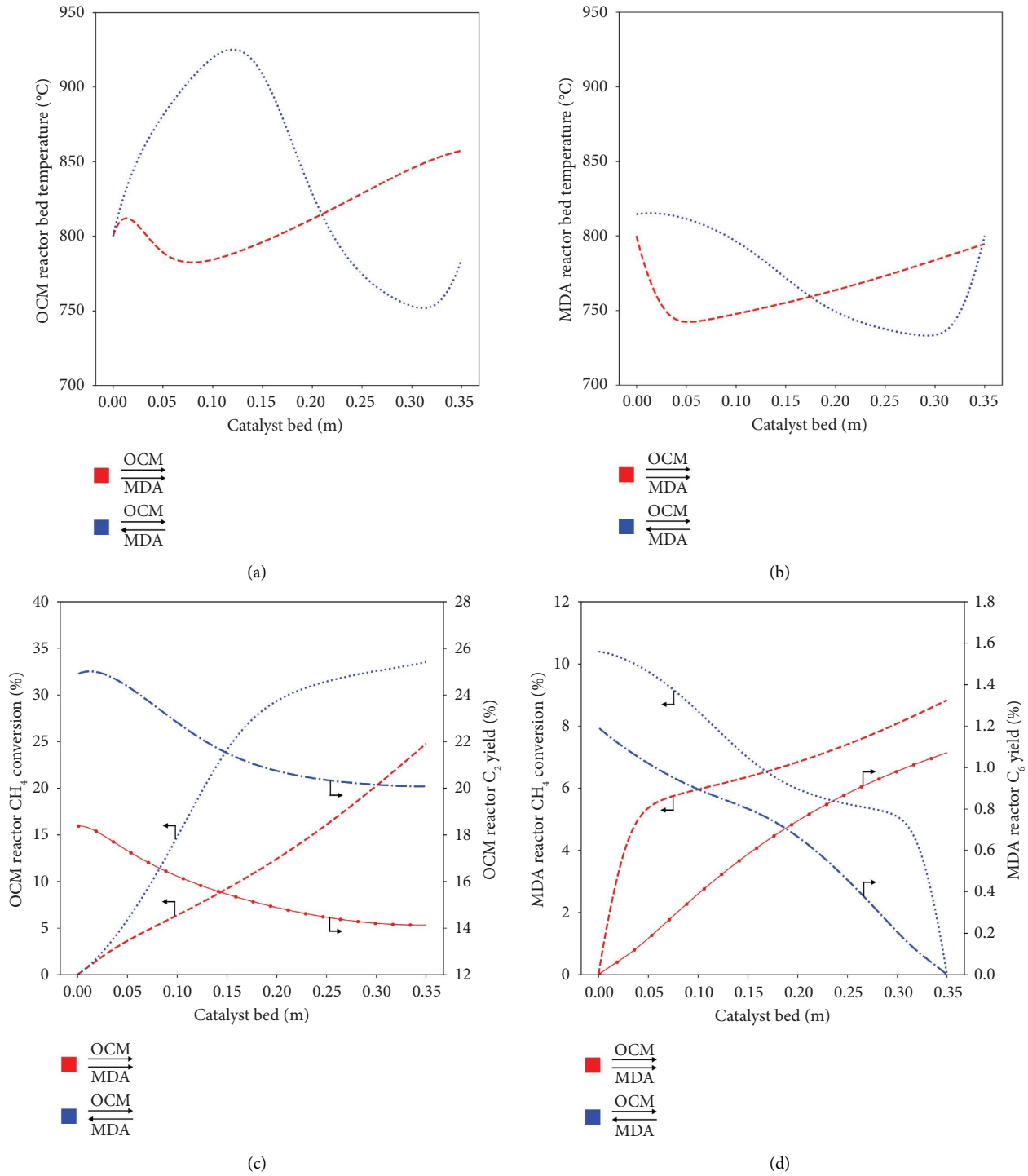
(a)

(b)

(c)

(d)

FIGURE 8: Comparison of a cocurrent (a and c) and countercurrent (b and d) reactor temperature and performance profiles at $U_{overall} = 800\,\text{W/m}^2.\text{K}$.

geometrical variations. This is a limitation of the used approach that needs to be addressed in the future. Computational fluid dynamics (CFD) is the best approach to use to study this geometrical variation and discriminate between these designs. CFD will also incorporate more accuracy in the heat transfer between the channel and incorporate axial

and back mixing phenomena that are critical for the OCM reactor design. OCM is a highly exothermic reaction and could have multiple steady-state solutions and the steady-state attained in a specific case depends on the start-up (or initial) conditions [26, 27]. CFD is also valuable to study different possible diluent profiling to optimize the reactor

TABLE 7: Results of the tabulated coupling methodology for case 1 in Table 8.

| | Input layer | | | Reactor optimizer | | Output layer | | | | |
Priority	Name	Units	Initial input	Constraints	Optimum input	Name	Units	Initial output	Optimum output	Targets
OCM	Optimization case									
1	Inlet temperature	°C	800	800	800	C_2 yield	%	10.1	41.3	>30
2	Inlet pressure	atm	1	1	1	CH_4 conv.	%	22.5	52.8	
3	Feed flow rate	Std m³/h	10,000	10,000	10,000	O_2 conv.	%	81.7	100.0	
4	Feed composition (CH4)	%	61.7	61.7	61.7	Reynold's no. (particle)	—	13.3	59.8	<20
5	Feed composition (inerts)	%	17.8	17.8	17.8	Δp (% of P_{in})	%	19.0	13.6	<100
6	Superficial velocity	m/s	2.6	0.2 – 3.5	3.9	T_{peak} ($T_{max} - T_{in}$)	K	21.9	84.3	
7	Particle dia.	mm	1	0.5 – 5.0	3.0	T_{lower} ($T_{in} - T_{min}$)	K	39.7	0.0	
8	Tube dia.	cm	0.8	0.5 – 30.0	1.9	σT	K	19.8	20.7	
9	Gas void fraction	—	0.5	0.5	0.5	Space time	sec	0.2	0.3	
10	Catalyst void fraction	—	0.5	0.01 – 0.5	0.5	Catalyst weight	kgs	78.0	121.9	
11	Flow direction	—	Cocurrent	Cocurrent	Cocurrent	No. of tubes	—	20000	1000	
12	Channel length	cm	45.0	5–100	100.0					
13	Tube wall thickness	mm	5.0	2–20	5.0					
14	$U_{overall}$	W/m².K	1000	1000–2500	1200					
MDA	Optimization case									
14	Inlet temperature	°C	800	800	800	C_6 yield	%	1.4	0.5	
15	Inlet pressure	atm	1	1	1	CH_4 conv.	%	9.6	10.0	10
16	Feed flow rate	Std m³/h	72,320	72,320	72,320	Reynold's no. (particle)	—	2.98	13.4	
17	Feed composition (inerts)	%	5	5	5	Δp (% of pin)	%	2.1	0.9	<20
18	Superficial velocity	m/s	0.5	0.2–3.5	0.8	T_{peak} ($T_{max} - T_{in}$)	K	1.2	9.3	<100
19	Particle dia.	mm	1.0	0.5–5.0	3.0	T_{lower} ($T_{in} - T_{min}$)	K	56.9	60.3	
20	Tube dia.	cm	6.3	0.5–30.0	21.8	σT	K	18.1	23.4	
21	Gas void fraction	—	0.5	0.5	0.5	Space time	sec	0.9	1.3	
22	Catalyst void fraction	—	0.5	0.1–0.5	0.5	Catalyst weight	kgs	4506	9086	

TABLE 8: Design parameters of autothermal coupled reactors according to targets in Table 7 and capacities in Figure 9.

| Showcase #	Reactor	L cm	d_{tube} cm	Tubes —	W_{cat} kgs	ε_d %	$U_{overall}$ W/m².K	T_p °C	T_L °C	$\Delta P/P_{in}$ %	τ sec	X_{CH4} %	X_{O2} %	$S_{C2/C6}$ %	$Y_{C2/C6}$ %
1*	OCM	100	3.0	1000	123	0	1200	84.3	0	13.6	0.3	52.8	100	78.2	41.3
	MDA		18.5		6667	0		9.3	60.3	0.9	1.3	11.1	—	18.4	2.0
2	OCM	100	18.4	1000	123	48.6	250	70.8	0	0.2	9.5	51.8	99.9	77.5	40.1
	MDA		25.9		6667	0		9.4	59.9	0.9	1.3	11.0	—	18.2	2.0
3	OCM	50	18.4	2000	123	48.6	250	71.1	0	0.1	9.5	51.8	99.9	77.5	40.2
	MDA		25.9		6667	0		9.5	59.9	0.3	1.3	11.0	—	18.3	2.0
4	OCM	200	18.4	500	123	48.6	250	69.7	0	0.1	9.5	51.6	99.9	77.5	40.0
	MDA		25.9		6667	0		8.5	59.9	0.3	1.3	11.0	—	18.0	2.0
5	OCM	25	11.6	10000	123	48.6	250	44.7	16.5	0.1	9.5	42.3	99.5	69.5	29.4
	MDA		16.4		6667	0		10.4	58.5	0.1	1.3	11.0	—	17.9	2.0
6	OCM	200	9.2	2000	123	48.6	250	37.9	27.0	0.6	9.5	38.7	100	65	25.1
	MDA		12.9		6667			10.7	58.0	4.7	1.3	11.1	—	17.7	2.0
7	OCM	100	20.6	1000	115	49.0	200	83.3	0	0.2	12.0	52.0	100	77.7	40.4
	MDA		27.5		6667	0		9.5	60.7	0.9	1.3	11.0	—	18.2	2.0
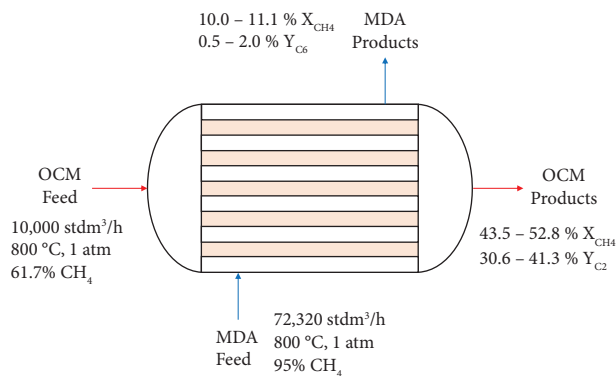
FIGURE 9: Example of an autothermal OCM-MDA coupled reactor with given inlet conditions and predicted result as ranges from different reactor geometrical variations similar to what is reported in Table 8.

and the influence of altering the diluent heat conductivity and other relevant physical properties to influence the heat transfer performance.

Case 7 is the last in Table 8 and is made to show that $U_{overall}$ can be further reduced to generate new design candidates. In this case, the $U_{overall}$ is reduced to 200 W/m^2.K but it needs more diluent. A similar performance as case 2 has been reached. However, the amount of OCM catalyst was reduced to 115 kg, as the peak temperature was slightly higher and complete O_2 consumption was reached. All the presented cases showed how critical is the $U_{overall}$ on the final design. The model used in this work is relatively simple. It was chosen because it is the first time that OCM and MDA coupling in the same reactor was investigated. Keeping the reactor model simple enabled the identification of potential operating windows for the design and generated many preliminary design candidates that can be investigated in more detail. This work also identified the possible mode of operation as cocurrent or countercurrent and the effect of diluent on thermal coupling. As this work seeks to generate initial candidates for OCM-MDA reactors, the code for the coupled reactor model used in this work is included in the supplementary material (available here). This will save effort and time to replicate this work and expand the model with more details in the future. Proposed future work should include using a realistic correlation to predict $U_{overall}$ value and account for axial and back mixing of mass and heat transfer especially for OCM side. Implement an advanced optimization algorithm to explore the entire design space and also to have a dynamic reactor model to study and evaluate the possible scenarios for safe startup and shutdown of such reactor design.

4. Conclusions

This work did a systematic modeling study to better understand the integration space between OCM and MDA in terms of opportunities and limitations. The focus was on thermal integration which serves as the foundation for the more attractive full mass and heat integration in the same reactor. Also, this work aimed to generate initial design

candidates for recuperative thermal coupled OCM-MDA reactors. To help support future work on these two reactions, the numerical code for the coupled reactor model used in this work is included in the supplementary material. The following findings have been achieved from this work.

(1) The separated reactors study was successful in defining the initial heat duty and amount of catalyst requirements. When operating OCM and MDA between 700 and 800°C temperature, 1–5 atm pressure, and an industrial scale feed throughput of GHSV 830–14,000 h^{-1} (10,000 to 20,000 m3(std)/h), the resulting heat duties are in the range of 1 MW to 13 MW. If this heat duty needs to be matched by both the reactors, the MDA catalyst needs to be 6 to 12 times larger than that of OCM. As well, the flow rate of the MDA reactor side needs to be 5 to 7 times larger than the OCM side.

(2) A systematic tabulated methodology is used to better structure and visualize the possible integration window. It is possible to integrate OCM and MDA in an autothermal reactor design. Pressure drop and space times were used to define representative dimensions for the tube-tube reactor model. The model was based on one reactor unit cell which can be replicated to achieve the target industrial flow capacity by numbering up so it will be a multitubular reactor design. Input data and conditions needed to set up the tube-in-tube autothermal reactor model were identified. The most critical design parameter was the overall heat transfer coefficient. It needs to be larger than 1000 W/m^2.K to avoid OCM thermal run when integrated with MDA. This value can be reduced by mixing the catalyst with diluent, but the reactor volume will increase. For one case study, it was possible to reduce the $U_{overall}$ from 1000 W/m^2.K to 200 W/m^2.K while keeping the same axial temperature profile when using 80% of the diluent in both MDA and OCM reactors. However, the reactor volume was increased by 5 times.

(3) The use of diluent proves valuable as a strategy to reduce the temperature variation in the axial direction. The best achieved axial temperature profile case was when the catalyst profiling is implemented in the MDA side from 0% to 100%, combined with the cocurrent operation. In all of the studied designs, the variations of temperature ((T_{peak}-T_{in}) or (T_{in}-T_{lower})) in the axial direction were less than 100°C for both the reactions. The axial temperature variation for the OCM sides was 3 times larger than that of the MDA side.

(4) The optimization was carried out manually in this work. This was a necessary initial step to understand the possible design integration window before aiming at ways to identify the most optimal design. A couple of design candidates were identified from this work based on an OCM feed capacity of 10000 m^3(std)/h at an inlet temperature of 800°C and

atmospheric pressure. The required MDA feed capacity was $72320 \, m^3$(std)/h which was fed with cocurrent OCM at the same operating conditions. Methane conversion was in the range of 43.5–52.8% and 10.0–11.1% for OCM and MDA, respectively. The design was performed with a C2+ yield larger than 30% and a benzene yield between 0.5 and 2.0% in OCM and MDA, respectively. The total amount of catalyst needed was 115 to 123 kg and 6667 kg for OCM and MDA, respectively. The total number of required OCM reactor tubes varied between 500 and 10000 with tube lengths between 0.25 and 2.0 m. The tube diameters for one reactor unit cell for OCM and MDA were in the range of 3.0–20.6 cm and 16.7–27.5 cm, respectively. These variations in dimensions and the number of parallel tubes required are the results of using diluents which influenced the axial temperature profile where the peak temperature to inlet temperature varied between 37.9 and 84.3°C.

Although some design candidates for the recuperative autothermal reactor design have been identified, this work was based on many assumptions which still need future follow-up work. The most critical aspects to be addressed are the overall heat transfer coefficient and ignoring the axial and back mixing of mass and heat transfer. These are best explored using CFD studies to optimize the diluents and geometrical design and validate the findings experimentally. The second is to use a more rigorous optimization method to identify the most optimal reactor design options. This needs to be supported with the experimental studies. Overall, this work is merely a starting point toward exploring the full potential of the coupling opportunities between OCM and MDA. It generated initial design candidates for autothermal reactor design and paves the path toward the more attractive full mass and heat integration in the same reactor.

Nomenclature

A_h: Heat exchanging surface, OCM side (cm^2), $A_h = 2\pi r_h l$
A_w: Heat exchanging surface, wall side, $A_w = 2\pi r_w l$
A_c: Heat exchanging surface, MDA side (cm^2), $A_c = 2\pi r_c l$
A_m: Log mean of A_h and A_c (cm^2), $A_m = (A_h - A_c)/(\log(A_h/A_c))$
A_{cs}: Cross-sectional area of the reactor tube (cm^2)
$C_{P,i}$: Specific heat capacity of component i ($J \, mol^{-1} \, K^{-1}$)
$\Delta C_{P,j,i}$: Delta specific heat capacity for reaction j with respect to component i ($J \, mol^{-1} \, K^{-1}$)
d_p: Catalyst particle diameter (cm)
F_i: Molar flowrate of component i ($mol \, h^{-1}$)
$H_{f,i}$: Enthalpy of formation of component i ($J \, mol^{-1}$)
$\Delta H_{j,i}$: Delta enthalpy of reaction j at temperature T ($J \, mol^{-1}$)
$\Delta H^o_{j,i}$: Standard delta enthalpy of reaction j at temperature T_R ($J \, mol^{-1}$)

h_h: Heat transfer coefficient for exothermic OCM side ($W \, m^{-2} \, K^{-1}$)
h_c: Heat transfer coefficient for endothermic MDA side ($W \, m^{-2} \, K^{-1}$)
k: Thermal conductivity of the gas ($W \, cm^{-1} \, K^{-1}$)
k_j: Reaction rate constant of reaction j (mol, atm, s, and cm^3)
k_{fj}: Forward rate constant of reaction j (mol, atm, h, g, and cat)
K_{pj}: Equilibrium constant of reaction j (atm)
m_s: Solid mass (g)
m_c: Catalyst mass (g)
m_d: Diluent mass (g)
Nu: Nusselt's number, $Nu = h_w(d_p/k)$
p_i: Partial pressure of component i (atm)
Pr: Prandtl number, $Pr = (C_p \mu/k)$
Q_g: Total heat generated by the reactions ($J \, cm^{-1} \, h^{-1}$)
Q_{ex}: Total heat removed from the reactor ($J \, cm^{-1} \, h^{-1}$)
R: Ideal gas constant
r: Tube radius (cm)
$r_{j,i}$: Rate of formation of component i in reaction j ($mol \, cm^{-3} \, s^{-1}$)
$r_{i,net}$: Net reaction rate for component I, equal to sum of rates of all reactions q in which i appears
Δr: Radius of the MDA packed bed (cm)
r_h: Inner tube radius of the OCM side (cm)
r_w: Outer tube radius of the OCM side (cm)
$R_{bed,h}$: Heat transfer resistance from the OCM reactor bed
$R_{bed,c}$: Heat transfer resistance from the MDA reactor bed
$R_{w,h}$: Heat transfer resistance near the OCM reactor wall
$R_{w,c}$: Heat transfer resistance near the MDA reactor wall
R_w: Heat transfer resistance from the diving wall
Re: Reynold's number, $Re = (\rho v d_p/\mu)$
T: Process side temperature (K)
T_R: Reference temperature, 298.15 (K)
$U_{overall}$: Overall heat transfer coefficient ($J \, cm^{-3} \, s^{-1} \, K^{-1}$)
v: Volumetric flowrate of the gas ($cm^3 \, s^{-1}$)
V_r: Reactor volume (cm^3)
V_v: Void volume (cm^3)
V_c: Catalyst volume (cm^3)
V_d: Diluent volume (cm^3)
Δw: Thickness of the dividing wall (cm)
X_i: Conversion of component (%), $X_i = (F_{i,in} - F_{i,out}/F_{i,in}) * 100$, and i: CH_4 and O_2
S_i: Selectivity of component (%), $S_i = iC * (F_{i,out}/F_{i,in} - F_{i,out})$, iC: number of carbons in the component i, and i: C_2H_4, C_2H_6, C_6H_6, and $C_{10}H_8$
Y_i: Yield of component i: CH_4, O_2, (%), Yield (i) %, and Y_i = Selectivity (i) * Conversion $(CH_4) * 100$
η_j: Approach to equilibrium
θ_a: Stoichiometric reaction coefficient of reference component a

θ_i: Stoichiometric reaction coefficient of component i

ρ: Gas density (g cm^{-3})

ρ_b: Bulk density (g cm^{-3})

ε_v: Void fraction

ε_c: Catalyst void fraction

ε_d: Diluent void fraction

λ_w: Thermal conductivity of diving wall (W cm^{-1} K^{-1})

μ: Gas viscosity (cm^2 s^{-1})

σT: Standard deviation of temperature $\sigma T = \sqrt{(\sum |T - T_{\text{mean}}|/N)}$, where N represents the total number of observations and T_{mean} represents the average temperature of the observations (°C).

Data Availability

The data used to support the findings of this study are available from the corresponding author upon request.

Conflicts of Interest

The authors declare that they have no conflicts of interest.

Acknowledgments

Supplementary Materials

This part has the numerical code for case 2 in Table 8. This code was developed and run using Python in JupyterLab version 3.4.4. (*Supplementary Materials*)

References

[1] L. Chen, Z. Qi, S. Zhang, J. Su, and G. A. Somorjai, "Catalytic hydrogen production from methane: a review on recent progress and prospect," *Catalysts*, vol. 10, no. 8, p. 858, 2020.

[2] M. A. Barteau, "Is it time to stop searching for better catalysts for oxidative coupling of methane?" *Journal of Catalysis*, vol. 408, pp. 173–178, 2022.

[3] K. Takahashi, J. Ohyama, S. Nishimura et al., "Catalysts informatics: paradigm shift towards data-driven catalyst design," *Chemical Communications*, vol. 59, no. 16, pp. 2222–2238, 2023.

[4] A. Cruellas, T. Melchiori, F. Gallucci, and M. van Sint Annaland, "Advanced reactor concepts for oxidative coupling of methane," *Catalysis Reviews*, vol. 59, no. 3, pp. 234–294, 2017.

[5] M. R. Rahimpour, M. R. Dehnavi, F. Allahgholipour, D. Iranshahi, and S. M. Jokar, "Assessment and comparison of different catalytic coupling exothermic and endothermic reactions: a review," *Applied Energy*, vol. 99, pp. 496–512, 2012.

[6] R. C. Ramaswamy, P. A. Ramachandran, and M. P. Duduković, "Recuperative coupling of exothermic and endothermic reactions," *Chemical Engineering Science*, vol. 61, no. 2, pp. 459–472, 2006.

[7] R. C. Ramaswamy, P. A. Ramachandran, and M. P. Duduković, "Coupling exothermic and endothermic reactions in adiabatic reactors," *Chemical Engineering Science*, vol. 63, no. 6, pp. 1654–1667, 2008.

[8] R. C. Brown, "Process intensification through directly coupled autothermal operation of chemical reactors," *Joule*, vol. 4, no. 11, pp. 2268–2289, 2020.

[9] V. Balakotaiah, Z. Sun, and D. H. West, "Autothermal reactor design for catalytic partial oxidations," *Chemical Engineering Journal*, vol. 374, pp. 1403–1419, 2019.

[10] P. Ferreira-Aparicio, M. J. Benito, and J. L. Sanz, "New trends in reforming technologies: from hydrogen industrial plants to multifuel microreformers," *Catalysis Reviews*, vol. 47, no. 4, pp. 491–588, 2005.

[11] H. Mimoun, A. Robine, S. Bonnaudet, and C. J. Cameron, "Oxidative coupling of methane followed by ethane pyrolysis," *Chemistry Letters*, vol. 18, no. 12, pp. 2185–2188, 1989.

[12] O. Kiyoshi and K. Takayuki, "Conversion of methane to aromatic hydrocarbons by combination of catalysts," *Chemistry Letters*, vol. 15, pp. 1955–1958, 1986.

[13] A. Obradović, J. W. Thybaut, and G. B. Marin, "Oxidative coupling of methane: opportunities for microkinetic model-assisted process implementations," *Chemical Engineering & Technology*, vol. 39, no. 11, pp. 1996–2010, 2016.

[14] J. Cizeron, G. Radaelli, L. Satish et al., "Reactors and systems for oxidative coupling of methane," United States Patent, Alexandria, VA, USA, US10047020B2, 2023.

[15] N. Elrefaei, N. Basha, M. Nounou, H. Nounou, A. Ashok, and M. Al-Rawashdeh, "Quantified database for methane dehydroaromatization reaction," *ChemCatChem*, vol. 14, no. 21, 2022.

[16] K. Skutil and M. Taniewski, "Indirect methane aromatization via oxidative coupling, products separation and aromatization steps," *Fuel Processing Technology*, vol. 88, no. 9, pp. 877–882, 2007.

[17] K. Skutil and M. Taniewski, "Some technological aspects of methane aromatization (direct and via oxidative coupling)," *Fuel Processing Technology*, vol. 87, no. 6, pp. 511–521, 2006.

[18] W. Wang and Y. S. Lin, "Analysis of oxidative coupling of methane in dense oxide membrane reactors," *Journal of Membrane Science*, vol. 103, no. 3, pp. 219–233, 1995.

[19] Y. Zhu, N. Al-ebbinni, R. Henney, C. Yi, and R. Barat, "Extension to multiple temperatures of a three-reaction global kinetic model for methane dehydroaromatization," *Chemical Engineering Science*, vol. 177, pp. 132–138, 2018.

[20] Adelq, "Thermochem 0.8.0," 2020, https://thermochem. readthedocs.io/_/downloads/en/latest/pdf/.

[21] M. Leva, "Packed-tube heat transfer," *Industrial and Engineering Chemistry*, vol. 42, no. 12, pp. 2498–2501, 1950.

[22] A. P. de Wasch and G. F. Froment, "Heat transfer in packed beds," *Chemical Engineering Science*, vol. 27, no. 3, pp. 567–576, 1972.

[23] A. G. Dixon and D. L. Cresswell, "Theoretical prediction of effective heat transfer parameters in packed beds," *AIChE Journal*, vol. 25, no. 4, pp. 663–676, 1979.

[24] E. Tsotsas and E. U. Schlünder, "Heat transfer in packed beds with fluid flow: remarks on the meaning and the calculation of

a heat transfer coefficient at the wall," *Chemical Engineering Science*, vol. 45, no. 4, pp. 819–837, 1990.

[25] S. V. Dimov, A. G. Sipatrov, N. A. Rudina, V. V. Kuznetsov, and A. A. Khassin, "Thermal conductivity of composite catalysts containing metallic copper as a reinforcing component," *Theoretical Foundations of Chemical Engineering*, vol. 41, no. 2, pp. 184–192, 2007.

[26] Z. Sun, D. H. West, and V. Balakotaiah, "Bifurcation analysis of catalytic partial oxidations in laboratory-scale packed-bed reactors with heat exchange," *Chemical Engineering Journal*, vol. 377, Article ID 119765, 2019.

[27] L. A. Vandewalle, R. Van de Vijver, K. M. Van Geem, and G. B. Marin, "The role of mass and heat transfer in the design of novel reactors for oxidative coupling of methane," *Chemical Engineering Science*, vol. 198, pp. 268–289, 2019.